LA-UR-12-20629
Approved for public release; distribution is unlimited.

Title: Hot Isostatic Press Manufacturing Process Development for Fabrication of RERTR Monolithic Fuel Plates

Author(s):
Crapps, Justin M.
Clarke, Kester D.
Katz, Joel D.
Alexander, David J.
Aikin, Beverly
Vargas, Victor D.
Montalvo, Joel D.
Dombrowski, David E.
Mihaila, Bogdan

Intended for: PowderMet2012, 2012-06-10/2012-06-13 (Nashville, Tennessee, United States)

LA-UR-12-2069

Hot Isostatic Press Manufacturing Process Development for Fabrication of RERTR Monolithic Fuel Plates

J. Crapps, K. Clarke, J. Katz, D. J. Alexander, B. Aikin, V. Vargas, J. Montalvo, D.E. Dombrowski, and B. Mihaila

Materials Science and Technology Division, Los Alamos National Laboratory
Los Alamos, New Mexico, USA

ABSTRACT

We use experimentation and finite element modeling to study a Hot Isostatic Press (HIP) manufacturing process for U-10Mo Monolithic Fuel Plates. Finite element simulations are used to identify the material properties affecting the process and improve the process geometry. Accounting for the high temperature material properties and plasticity is important to obtain qualitative agreement between model and experimental results. The model allows us to improve the process geometry and provide guidance on selection of material and finish conditions for the process strongbacks. We conclude that the HIP can must be fully filled to provide uniform normal stress across the bonding interface.

INTRODUCTION

The United States Department of Energy, Office of the National Nuclear Security Administration, established the Global Threat Reduction Initiative (GTRI) program in the office of Defense Nuclear Nonproliferation to reduce and protect vulnerable nuclear and radiological material located at civilian sites worldwide by providing support for other countries own national programs. An important component of the GTRI is the need to convert research reactors from the use of highly enriched uranium (HEU) to low-enriched uranium (LEU), with less than 20% uranium enrichment. These efforts result in permanent threat reduction by minimizing and, to the extent possible, eliminating the need for HEU in civilian applications.

Dispersion fuels made from LEU are inadequate for many high power test reactors [1]. To achieve the needed loading for high power test reactors, monolithic U-Mo alloy fuels have been proposed [2]. This introduces a new challenge of bonding aluminum cladding to monolithic fuels by processes other than the roll bonding traditionally used for dispersion fuels[2, 3].

The history of the fuel development process is discussed elsewhere [4]. Fuel foils are produced by a combination of hot and cold rolling processes and the cladding is applied via a hot isostatic press (HIP) process. The HIP process was selected because it produced the most consistent results when compared to high temperature rolling, friction bonding, and transient liquid phase bonding[3, 5]. HIPping requires that the components be contained in a can evacuated of atmosphere to prevent the formation of an oxide layer on the material surfaces which interferes with bonding.

In this work, we develop and experimentally validate a finite element model considering a longitudinal cross section of the HIP process using the finite element code ABAQUS. We use this model to learn

about the HIP process and component behavior during HIPping. The model shows that filling the HIP can aids in preventing excessive aluminum extrusion which causes insufficient cladding coverage over part of the fuel plate. We also show that a full can improves the distribution of normal stresses, reduces waviness of finished plates and promotes even bonding of cladding and fuel.

HIP PROCESS

During the HIP process, the fuel and cladding must be enclosed in an evacuated environment to keep the pressurized media (argon gas) from interfering with the bonding process. A 304 stainless steel can is used to provide this atmosphere free environment. Preparation of the can components is discussed elsewhere [6, 7].

The HIP can is composed of two cover plates, two side plates, a bottom plate, and top plate. Once assembled, the plates are joined via tungsten inert gas (TIG) welding to create a can with one cover plate unattached. The open HIP can is then loaded with alternating layers of rectangular steel plates called strongbacks and fuel plates composed of zirconium-clad U-10Mo foils and 6061-T6 aluminum cladding. To prevent movement of the U-10Mo foil during assembly and transport of the can, a pocket is machined into one side of the Al 6061-T6 cladding for the foil. The final cover plate is TIG welded in an argon filled glove box and the assembly is evacuated and sealed with a crimp weld. Figure 1 is a drawing of the fuel plates and strongbacks and Fig. 2 is a drawing of the HIP can components.

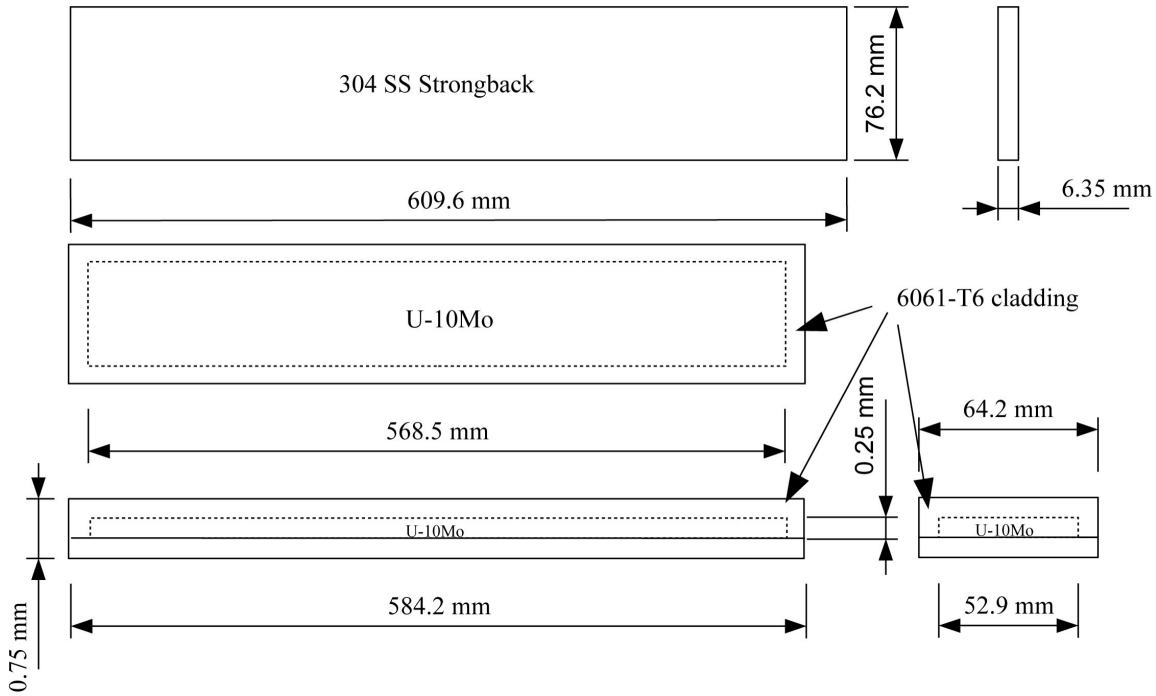

Figure 1. Fuel plates and strongbacks [4].

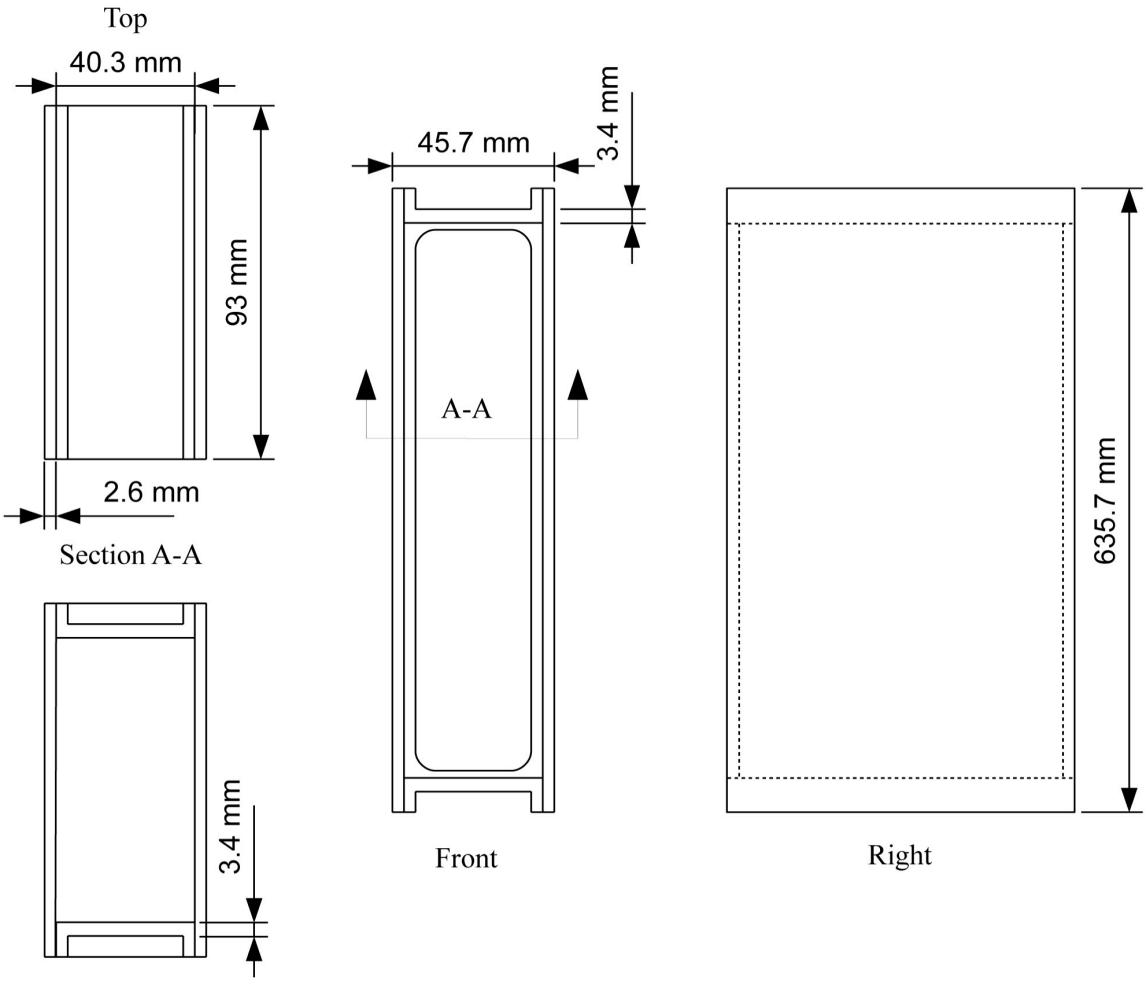

Figure 2. HIP can baseline design [4].

During the HIP process, the goal is to create aluminum-aluminum bonds around the perimeter of the fuel foil and aluminum-zirconium bonds elsewhere. The strongbacks are intended to minimize distortion of the fuel foil and cladding, producing a straighter clad fuel product. To prevent bonding of the strongbacks, aluminum, and can we use a parting agent. The preparation process for the U-10Mo foils and cladding is described elsewhere [7, 8].

The standard HIP processing steps are as follows: The assembled and evacuated HIP can is placed inside a HIP chamber and is heated to 320 ^{o}C (608 ^{o}F). Next, the HIP chamber is pressurized to 104.4 MPa (15 ksi) using argon gas while the temperature is raised to 560^{o}C (1040 ^{o}F) [6, 9]. The assembly is held at this temperature for 90 minutes after which the pressure is reduced to atmospheric and the assembly is allowed to cool for approximately two hours to room temperature. After the HIP process, the can is cut open and the components are removed. If the parting agent is well distributed, the aluminum foils separate from the strongbacks with minimal effort.

FINITE ELEMENT MODEL

We use ABAQUS CAE to create and execute the finite element models for this study and consider a two-dimensional model of a transverse cross section located at the center of the HIP can (long axis of can is normal to the plane of analysis). The HIP can, strongbacks, fuel foil, and cladding are modeled individually as deformable components assembled as shown by Fig 3.

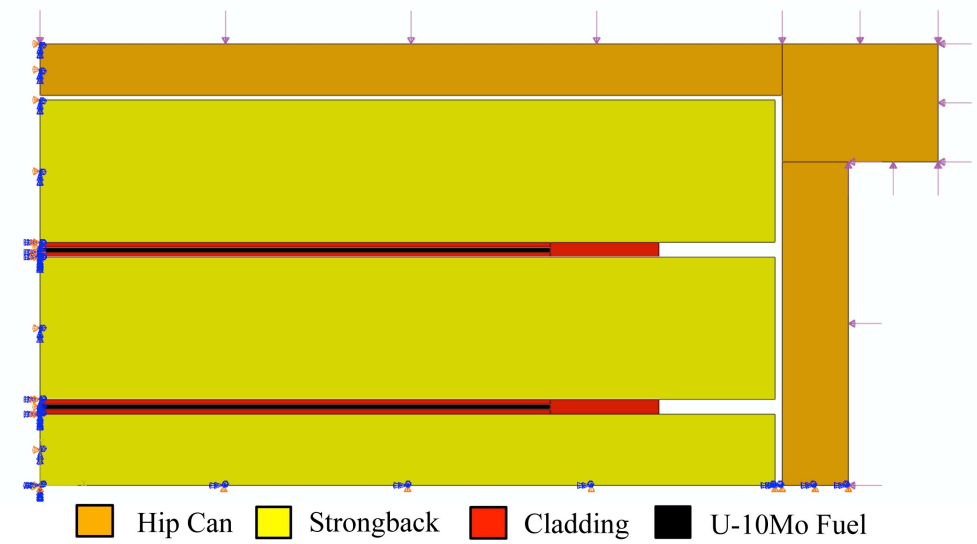

Figure 3. HIP can component assembly and boundary conditions [4].

For simplicity and computational efficiency, symmetry considerations are used to model one quarter of the assembly. We apply isostatic pressure to the outside surfaces of the HIP can as shown by Fig. 3. The isostatic pressure is applied to the HIP can in multiple steps to aid in contact detection. Initially, the pressure is increased by small increments until contact between the can and internal components is established. Afterward, the pressure is incremented by larger amounts to the desired pressure of 104.4 MPa (15 ksi). A single node was fixed on the vertical symmetry line (Fig. 3) to assure numerical stability while the HIP can deforms to contact the strongbacks and fuel plate stackup. Once contact was established, the fixed node was released.

We consider two materials in the finite element model: Al 6061-T6 and 304L stainless steel. The HIP process temperature is 560 ^{o}C (1040 ^{o}F). To explore the impact of properties used on simulation results, simulations are performed using the room and high temperature material properties given by Table 1. Al 6061-T6 high temperature material properties are not available, so we used data from the highest temperature available (371^{o} C) (700 ^{o}F). The solidus temperature of Al 6061 is 580 ^{o}C (1076 ^{o}F) and it is expected that after the HIP cycle, the aluminum is at or beyond an O-temper state after 90 min at 560 ^{o}C (1040 ^{o}F). The ABAQUS Mises plasticity model was used for all components in the analysis. A convergence study was conducted to ensure the accuracy of the simulation results.

Table 1. Material Properties [10, 11]

Material	Temp (^{o}C)	E (GPa)	Sy (MPa)	Su (MPa)	%el
304L SS	RT	193	186	482	42
304L SS	560	152	117	310	58
Al 6061-T6	RT	70	275	310	20
Al 6061-T6	371	47	12.4	20.6	98

The two-dimensional model of the HIP can is composed of hybrid plane strain elements with reduced integration (CPE4RH). The formulation of this element type includes an additional term relating to constant pressure. This formulation is recommended for improved convergence of simulations where the material is likely to extrude, but is constrained. The baseline simulation contains approximately 80,000 elements and takes about 40 min wallclock time using a single core of an Intel Xeon X5570 processor at 2.93 GHz. To decrease computational time, simulations can be executed on parallel processors.

Simulations are executed using 4 processors in parallel processing which was determined to be the most efficient use of computing resources as shown by Fig 4.

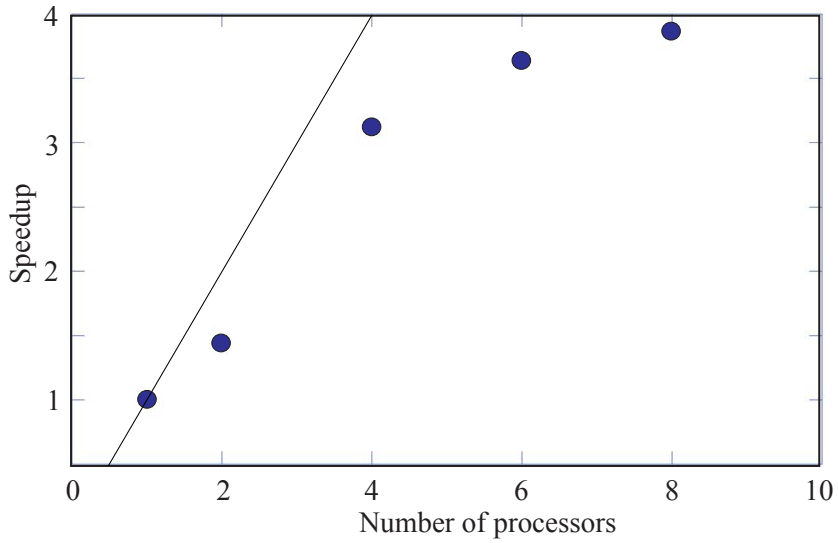

Figure 4. Simulation speedup as the number of processors is increased. The simulation considered elastic and plastic deformation in both the aluminum and steel at room temperature. Optimal computational efficiency occurs when using 4 processors.

Model sensitivity to material properties

Several cases considering elastic or elastic-plastic material behavior at room and high temperature were explored to investigate the importance of modeling different aspects of material behavior. Figures 5 and 6 illustrate the S22 contours and displacements for simulations considering an elastic response in all materials, elastic-plastic response in the aluminum, elastic-plastic response in the steel, and elastic-plastic response in the aluminum and steel for room and high temperature material properties. In these simulations, a friction coefficient of 0.1 was assumed.

Figure 5 shows that modeling the steel plasticity in the HIP can components at room temperature is important, while modeling plasticity in the aluminum cladding has a small effect. As the isostatic pressure increases to its maximum value (104.4 MPa) the steel in the corners of the HIP can yields due to bending stress, affecting the normal stresses along the bonding line of the U-Mo fuel and cladding. At room temperature, neither the cladding or fuel yield and remain in the elastic range after the full pressure of 104.4 MPa has been applied.

At elevated temperature, the yield strength (Sy), ultimate tensile strength (Su), and elastic modulus (E) decrease in both the aluminum (cladding) and the steel (can, strongbacks, and fuel surrogate). Figure 6 shows that modeling plasticity in both the aluminum and steel at elevated temperature (560 ^{o}C) has a strong effect on the stress normal to the bond line. To accurately simulate the process, the model needs to consider elastic and plastic material behavior close to the processing temperature.

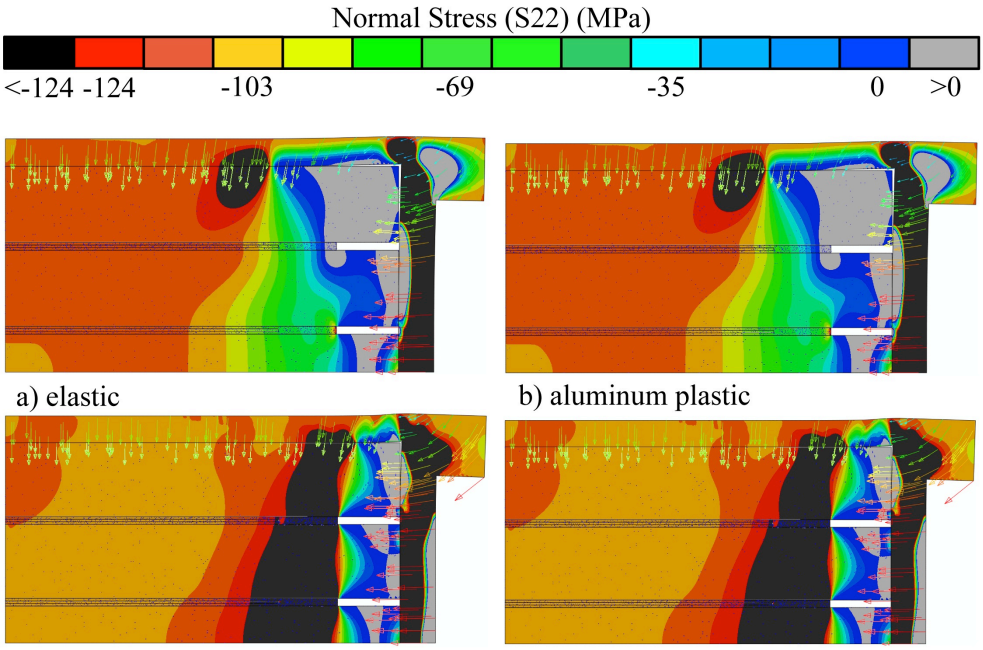

Figure 5. Stress contours and expected displacements (arrows) for baseline simulation at room temperature considering (a) fully elastic materials, (b) aluminum plasticity, (c) steel plasticity, and (d) steel and aluminum plasticity. Considering plasticity in the aluminum cladding does not influence the normal stress (S22) distributions.

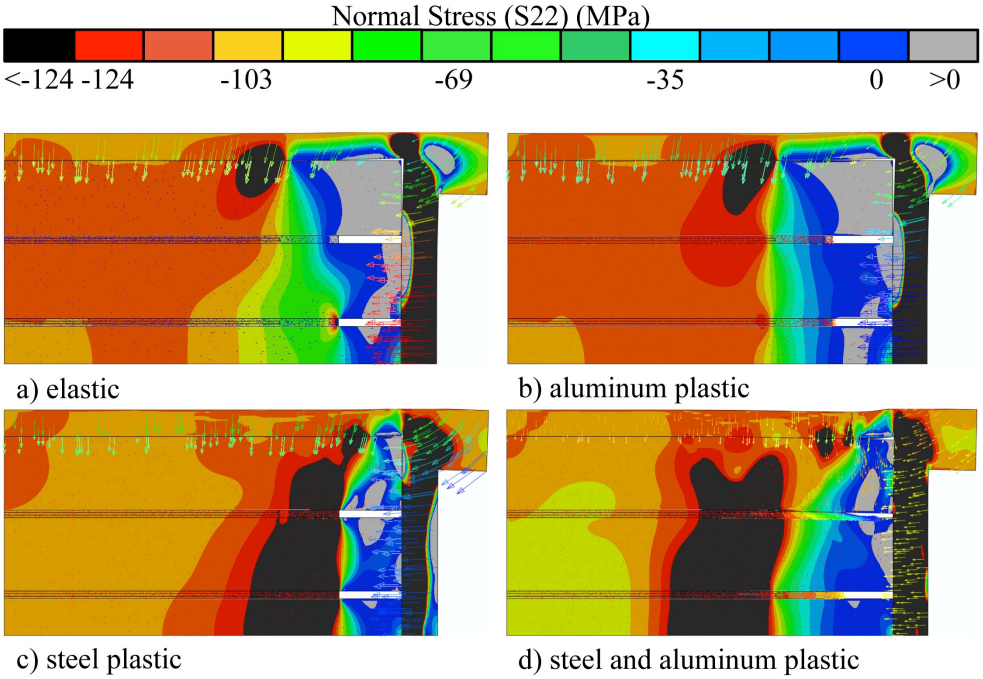

Figure 6. Stress contours and expected displacements (arrows) for baseline simulation at high temperature considering (a) fully elastic materials, (b) aluminum plasticity, (c) steel plasticity, and (d) steel and aluminum plasticity. Considering plasticity in both the steel and aluminum cladding has a strong effect on the normal stress (S22) distributions.

Model sensitivity to friction effects

The effect of considering friction effects was explored using a simple Coulomb friction model. Friction was defined for every contacting interface. Simulations were performed considering the baseline geometry with friction coefficients of 0.1, 0.3, and 0.6 and high temperature elastic-plastic material behavior. 0.1 was chosen as the minimum value of friction coefficient because of convergence issues due to unrestrained flow of the aluminum cladding in the case considering no friction. Figure 7 shows the simulation results. Friction has a small influence on the normal stress contours. Thus, controlling friction is not expected to improve the normal (bonding) stresses along the aluminum fuel interface. It is noted though that a low friction coefficient (Fig. 10a) is most consistent with the experimental results, which indicate that the aluminum cladding extrudes into the gaps between the strongbacks in the baseline case where the can is not filled.

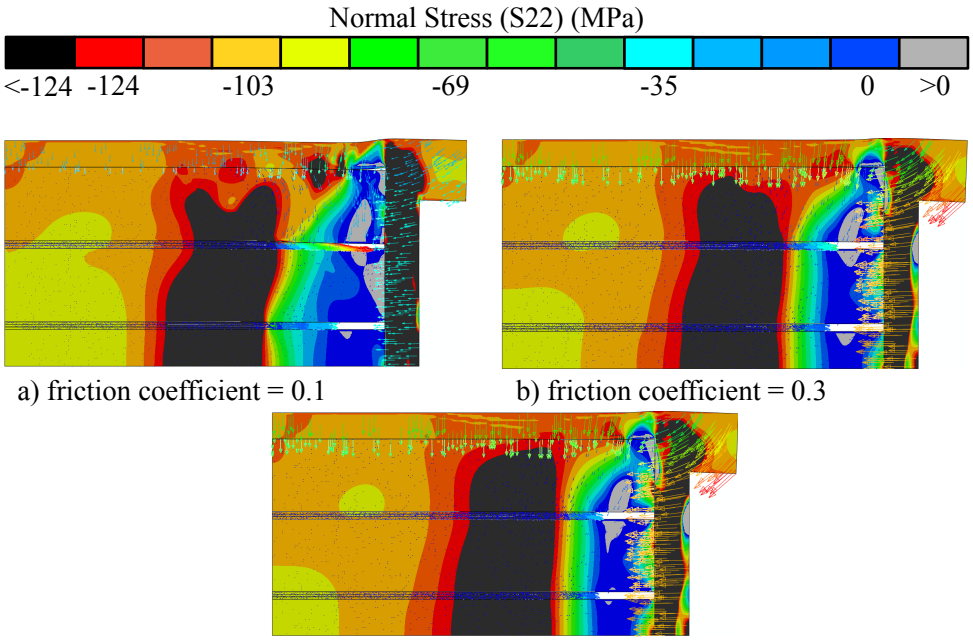

Figure 7. Normal stress contours and expected displacements (arrows) for simulations considering friction coefficients of 0.1, 0.3, and 0.6. The friction coefficient has a weak influence on the HIP model.

MODIFIED HIP CAN DESIGN

Based on the simulation results presented in Figs. 5, 6, and 7, we note the original HIP can design leads to three areas of concern in the HIP fuel-cladding bonding process:

1. Considerable extrusion of aluminum into the gap between the strongbacks will cause insufficient cladding coverage of the fuel plate.
2. The uneven distribution of normal stresses in the fuel-cladding bonding region will lead to uneven deformation (waviness) of the fuel plate.
3. The uneven distribution of normal stresses along the fuel-cladding interface is expected to give rise to uneven bonding of fuel to cladding.

These numerical findings are confirmed by results of experimental trials discussed in the experimental section.

Using a finite element model allows exploration of design changes in the HIP can geometry in order to improve the uniformity of the normal stresses along the fuel-cladding interface. This type of study will

reduce the time and cost that would be required to explore geometry modifications experimentally via a trial and error approach.

Figure 8 illustrates the normal stress distributions and expected displacements corresponding to two proposed modifications in the HIP can geometry. These changes are intended to reduce aluminum extrusion and improve the uniformity of the normal stress distribution along the fuel-cladding interface. In Fig. 8 we show (a) the results corresponding to the original HIP can design, (b) a modification of the HIP can geometry by extending the aluminum cladding to fill the space between the strongbacks, and (c) a second modification of the HIP can geometry by extending the width of the can, strongbacks, and aluminum cladding to an internal width of 5 in. In all cases, the dimensions of the fuel foil are left unchanged. Details of the behavior of the fuel plates in each of the situations shown by Fig. 8 are shown in Fig. 9.

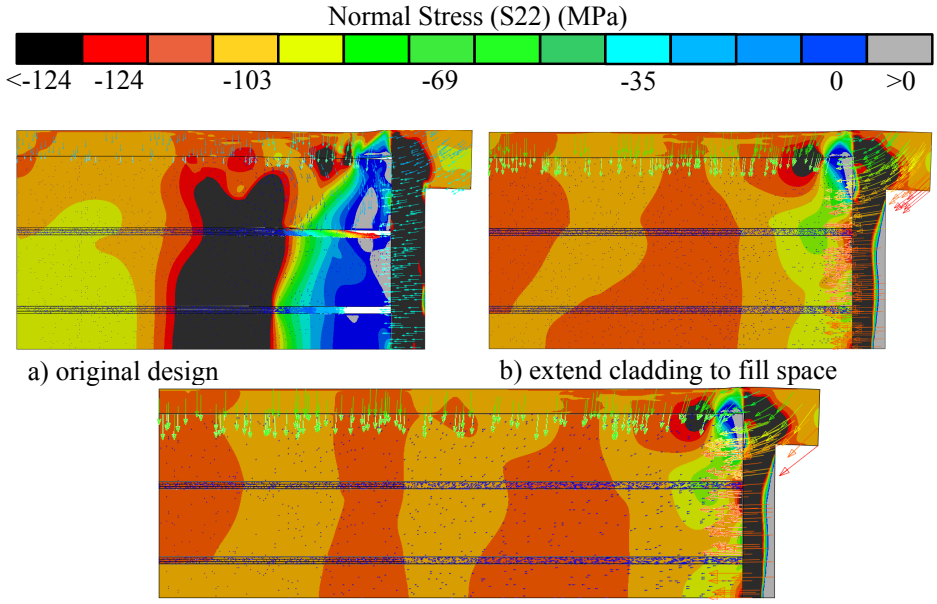

Figure 8. Normal stress contours and expected displacements (arrows) for two HIP can design modifications, compared with the original design (a). The aluminum cladding was extended to fill the original HIP can to aid in preventing aluminum extrusion (b). The HIP can and cladding width were both increased to 5 inches to improve the distribution of normal stresses along the fuel-cladding interface (c).

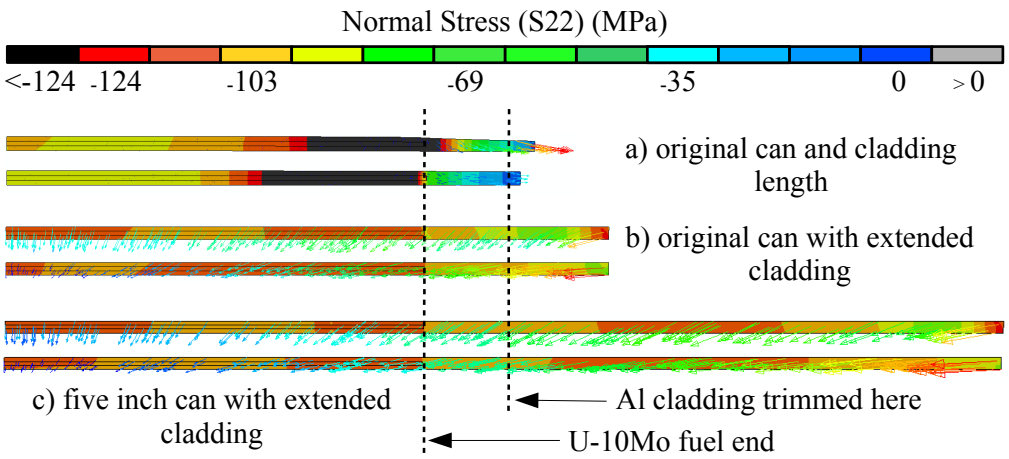

Figure 9. Fuel plate normal stress (S22) contours and expected displacements (arrows) for the two HIP can design modifications (b) and (c) shown in Fig. 11, compared with the original design (a). Excessive extrusion of the aluminum cladding can be prevented by extending the cladding to fill the can.

We conclude that the extrusion of the aluminum cladding into the gaps between the strongbacks can be significantly reduced by extending the cladding to fill the HIP can. Figures 8 (a) and (b) also show that extending the aluminum to fill the gap between the strongbacks significantly improves the normal stress distribution uniformity which will result in a flatter fuel-clad product. Extending the width of the can as shown in case (c) offers only a small improvement in the normal stress distribution along the fuel-cladding interface.

The original HIP can design considers four fuel plates in a single can (two are shown in a quarter symmetry model). We wish to investigate how many fuel plates can be put into a single HIP can and how the stress distribution changes as the total stackup height changes. Figure 10 illustrates how the normal stress distribution changes as four, six, eight, and ten fuel plates are processed in a single HIP can. The general trend shown in Fig. 10 is that as fuel plates are added to the HIP can, the stresses in the middle of the can become lower. Because these stresses are integral to creating a reliable bond, this is an undesirable situation because the bond between the fuel and cladding on all the plates may not be of consistent strength. The maximum number of plates that should be processed in the current HIP can design is six.

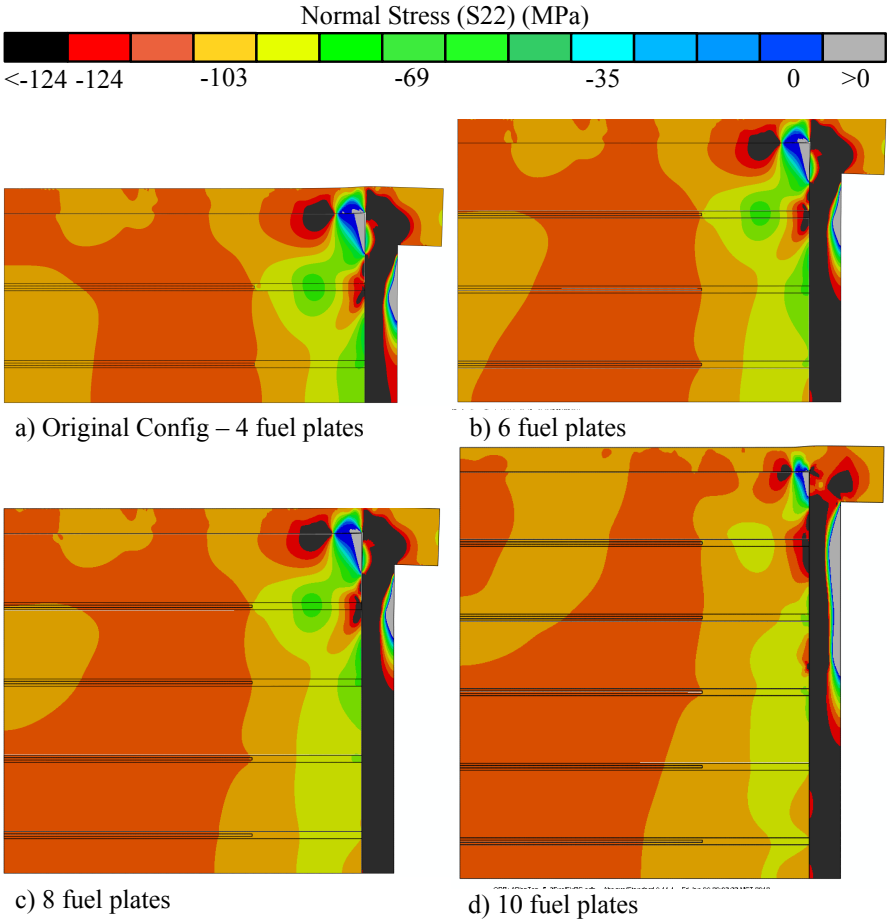

Figure 10. Processing additional fuel plates in HIP can: (a) original design; (b) 6 fuel plates; (c) 8 fuel plates; and (d) 10 fuel plates. The general trend when fuel plates are added to the HIP can is that the normal stresses along the center of the HIP can (bottom of pictures a-d) are relieved. This could cause weaker bonding at the end of the fuel plate and is an undesirable result.

EXPERIMENTS

Several HIP cans of the design shown by Figs. 1 and 2 were processed following the HIP process described earlier to determine the effects of stongback and fuel configuration within the can. Here we discuss cases considering aluminum cladding widths of 64.2 mm (2.53 in.) and 76.2 mm (3 in.). Experiments using the original HIP can design characterized by fuel plates with width and length significantly less than the strongback dimensions showed effects inferred from our finite-element simulatons including significant lateral aluminum extrusion and uneven distribution of aluminum cladding around the fuel. In addition, experiments demonstrated plastic deformation of the strongbacks, which precludes reusing the strongbacks in subsequent HIP cycles. The aluminum cladding extrusion and plastic deformation of the strongbacks reinforce the importance of modeling the HIP process within an elasto-plastic framework. Friction is important for the reliability of the model predictions and direct comparison of simulation and experimental results favors a small friction coefficient. Figure 11 shows the base and tube ends (i.e. the bottom and top extremities of the HIP can) for two HIP trials. Here, test 1 corresponds to a trial performed using the original HIP can while test 2 corresponds to a modified geometry with aluminum cladding being extended to fill the gap between the strong backs and the can (Figs 8b and 9b).

Increasing the size of the fuel plate relative to the size of the strongbacks dramatically improves the overall uniformity of the compression of the inserted stackup. We show in Fig. 11(b) the as removed base end of a HIP can stackup (five strongbacks and four fuel plates) with fuel plates that were 12.7mm (0.5in.) narrower and 25.4 mm (1 in.) shorter than the strongbacks. In Fig. 11(d), the as-removed base end of a HIP can stackup (five strongbacks and four fuel plates) with fuel plates the same width and length as the strongbacks is shown. The strongbacks shown in Fig. 11(a) show significant deformation. In the test1 experiment, the fuel plates shifted both vertically and horizontally in the HIP can. The extra space in the HIP can allows for the deformation of the strongbacks and movement of the fuel plates after assembly. In addition, significant extrusion of the aluminum cladding causes insufficient coverage of the fuel. Figure 11(c) shows that filling the HIP can by extending the aluminum cladding to match the strongback's dimensions reduces the uneven deformation of the strongbacks. Filling the can eliminates extrusion of all but a negligible volume of aluminum cladding.

Figure 12 shows transverse metallographic cross sections illustrating the uneven cladding and relative aluminum shifting encountered in the original HIP can design. Figures 12(a) and 12(c) show the edges of the as-removed fuel plates, corresponding to the tube ends in the tests depicted in Fig. 11 (b) and (d). Figure 12(b) and (d) show the transition region between aluminum-aluminum bonding at the edges and aluminum-zirconium bonding in the fuel plate regions at the same ends. When the HIP can is not filled, the final dimensions (overall and cladding thickness) of the fuel plate are not uniform. In contrast, when the aluminum cladding is extended to fill the gaps, dimensional accuracy is dramatically improved and metallograpy shows that the aluminum-aluminum and the fuel-cladding bonds are consistently sound.

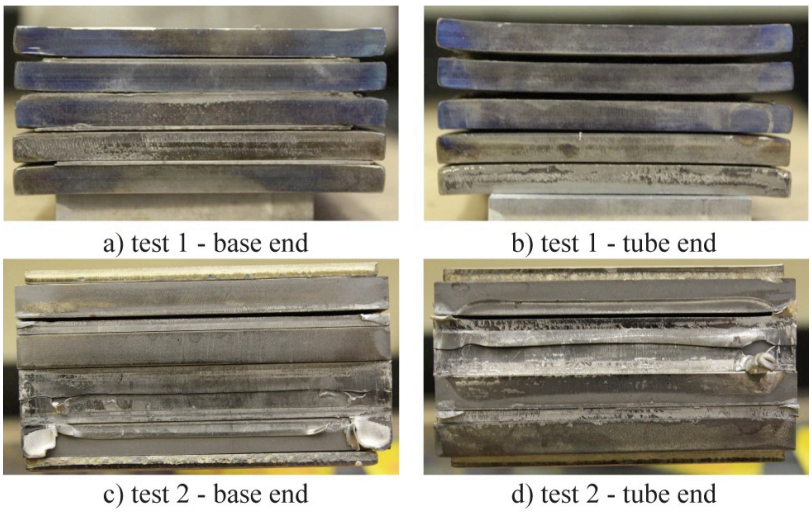

Figure 11. Base and tube ends of plate stackups (strongbacks and fuel plates) are shown as-removed from the HIP cans for: (test1) – aluminum cladding width is less than the strongback, showing uneven distribution of fuel plates from side to side, and from end to end; the fuel plates slide down toward the base of the can; (test2) – aluminum cladding and strongbacks have the same width, showing flat fuel plates filling the spaces between strongbacks have eliminated shifting.

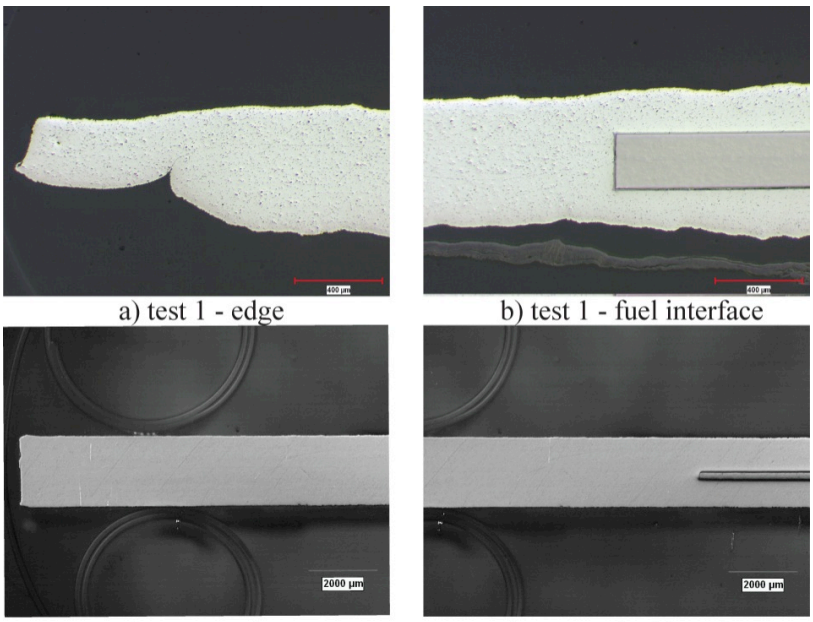

Figure 12. Transverse metallographic cross-sections of clad fuel after the HIP process in the two tests depicted in Fig. 10. Panels (a) and (c) show the edge of the aluminum cladding (b) and (d) show the corresponding ends of the fuel plate inside the cladding. In test 1, corresponding to a can which is not filled, metallography shows aluminum extrusion and uneven cladding. In test 2, corresponding to a filled HIP can, metallography shows a fuel plate with even cladding coverage and minimal extrusion.

CONCLUSIONS

Finite element simulation and experimentation were used to understand and improve the HIP manufacturing process for monolithic fuel plates. We show that the simulation results are sensitive to the temperature dependence of the material properties. For the steady state simulations considered here, it is important to use material properties close to the process temperature. Furthermore, plasticity for all components in the HIP can must be accounted for to obtain accurate predictions. The simulation results show that the HIP process is insensitive to the value of the friction coefficient, but a small friction coefficient is required to assure good qualitative agreement with experiments.

Use of the developed simulation showed that the maximum number of fuel plates that should be processed in the present HIP can design is six. Most importantly, our simulations indicate that extending the aluminum cladding to fill the space between the strongbacks prevents cladding extrusion into the space between strongbacks and aids in a more uniform distribution of normal stresses along the fuel-cladding interface. We experimentally verified that this change in geometry does lead to flat clad-fuel products. In addition, the plastic deformation of the steel strongbacks is dramatically reduced when the aluminum is extended to fill the HIP and these strongbacks can be reused in subsequent HIP runs.

ACKNOWLEDGEMENTS

Work performed in part under the auspices of the U.S. Department of Energy, Office of the National Nuclear Security Administration, under the Global Threat Reduction Initiative Reactor Convert program.

REFERENCES

[1] C. R. Clark, G. A. Moore, B. H. Park, J. F. Jue, N. P. Hallinand, and D. E. Burkes, "Monolithic fuel fabrication process development," presented at the 10th International Topica Meeting on Research Reactor Fuel Management, Sofia, Bulgaria, 2006.

[2] C. R. Clark, G. A. Moore, B. H. Park, J. F. Jue, N. P. Hallinand, and D. E. Burkes, "Update on monolithic fuel fabrication methods," presented at the RERTR 2006, 28th International Meeting on Reduced Enrichment for Research and Test Reactors, Cape Town, South Africa, 2006.

[3] C. R. Clark, G. A. Moore, G. C. Knighton, J. F. Jue, and J. M. Wight, "Update on monolithic fuel fabrication development," presented at the RERTR 2005, 27th International Meeting on Reduced Enricment for Research and Test Reactors, Boston, MA, 2005.

[4] J. Crapps, K. Clarke, J. Katz, D. J. Alexander, B. Aikin, V. Vargas, J. Montalvo, D. E. Dombrowski, and B. Mihaila, "Development of the hot isostatic press manufacturing process for monolithic nuclear fuel," *Submitted, Nuclear Engineering and Design,* 2011.

[5] A. B. Robinson, G. S. Chang, D. D. Keiser, D. M. Wachs, and D. L. Porter, "Irradiation performance of U-Mo alloy based 'momolithic' plate-type fuel - design selection," Idaho National Lab2009.

[6] J. F. Jue, B. H. Park, C. R. Clark, G. A. Moore, and D. D. Keiser, "Fabrication of monlithic RERTR fuels by hot isostatic pressing," *nuclear technology,* vol. 172, p. 6204, 2010.

[7] G. A. Moore, F. J. Rice, N. E. Woolstenhulme, W. D. Swank, D. C. Haggard, J. Jue, B. H. Park, S. E. Steffler, N. P. Hallinand, and M. D. Chapple, "Monolithic fuel fabrication process development at the idaho national laboratory," presented at the RERTR 2008, 30th International Meeting on Reduced Enrichment for Research and Test Reactors, Washington, DC, 2008.

[8] G. A. Moore, F. J. Rice, N. E. Woolstenhulme, J. F. Jue, B. H. Park, S. E. Steffler, N. P. Hallinand, M. D. Chapple, M. C. Marshall, and B. I. Mackowiak, "Monolithic fuel fabrication process deveopment at the Idaho National Laboratory," presented at the RERTR 2009, 31st International Meeting on Reduced Enrichment for Research and Test Reactors, Beijing, China, 2009.

[9] H. Ozaltun and P. G. Medvedev, "Structural behavior of monolithic fuel plates during hot isostatic pressing and annealing," presented at the 14th International Topical Meeting on Research Reactor Fuel Management, Marrakech, Morroco, 2010.

[10] *Aluminum Standards and Data*: The Aluminum Association, 1997.

[11] M. F. Rothman, *High-temperature property data: ferrous alloys*. Metals Park, OH: American Society for Metals, 1987.